Transient resonance Rayleigh scattering from electronic states in disordered systems: Excitons in GaAs/Al$_x$Ga$_{1-x}$As multiple-quantum-well structures

H. Stolz, D. Schwarze, and W. von der Osten

Fachbereich Physik, Universität-Gesamthochschule, Warburger Strasse 100A, D-4790 Paderborn, Federal Republic of Germany

G. Weimann

Walter Schottky Institut, Technische Universität München, D-8046 Garching, Federal Republic of Germany

Resonance Rayleigh scattering from electronic states in materials with static disorder is investigated both theoretically and experimentally. By using classical scattering theory we prove that this process, if excited by short optical pulses, decays with finite time constant determined by the coherence time or, equivalently, the homogeneous linewidth of the state. Experiments with picosecond time resolution at the ($n = 1$, e-hh) exciton in GaAs/Al$_x$Ga$_{1-x}$As multiple-quantum-well structures confirm this prediction. Exploiting the selection rules, from transient scattering the coherence time and energy-relaxation time are determined and measured as functions of exciton energy across the inhomogeneously broadened exciton band.

I. INTRODUCTION

The investigation of dephasing processes of optically excited states in solids has recently become an active and fast progressing field of research. Using various advanced laser spectroscopic techniques, these processes have been studied both in crystalline and in amorphous material systems (for recent reviews and references, see, e.g., Refs. 1–3). The important quantity to be extracted from the measurements is the homogeneous linewidth δE_{hom} or its equivalent, the coherence time τ_{coh} of the optical transition. Defining δE_{hom} as full (energy) width at half maximum (FWHM) of the homogeneous absorption line shape, it may be written in the form

$$\delta E_{hom} = 2\hbar/\tau_{coh} = 2\hbar(1/2T_1 + 1/T_2') . \tag{1}$$

Here, τ_{coh} (identical with the optical dephasing time often denoted by T_2) represents the average time during which the ensemble of excited states loses phase information. T_1 denotes the (total) energy relaxation time. Resulting in a depopulation of the states with rate $1/T_1$, it takes into account all *inelastic* processes such as radiative recombination, phonon scattering, and others. *Elastic* processes, on the other hand, contribute through $1/T_2'$ where T_2' is the "pure" dephasing time as usually introduced.

As implied by Eq. (1), measurements to determine δE_{hom} can be performed either in the frequency or in the time domain depending on the investigated system. In solids, the homogeneous linewidth is commonly obscured by more or less pronounced inhomogeneous broadening effects and therefore is not accessible to direct linewidth measurements. Still, information on δE_{hom} can often be obtained from spectral investigations such as fluorescence line narrowing or spectral hole burning.[1] These techniques eliminate the inhomogeneous width and were frequently employed to explore the dephasing mechanisms in doped organic and inorganic glasses. On the other

hand, the development of coherent transient techniques with picosecond and subpicosecond time resolution has permitted measurements in the time domain from which τ_{coh} is directly obtained and δE_{hom} can be deduced.[2,3] Among the methods of this second type are time-resolved degenerate four-wave mixing,[4–7] photon echoes,[8,9] transient absorption correlation,[10] and, most recently, quantum beat spectroscopy.[11–14] All were especially used in the investigation of dephasing processes of excitonic states in various crystals.

A direct and conceptually straightforward technique to measure coherence times of excited states is *resonant Rayleigh scattering* which up to now was hardly made use of. This kind of scattering process is well known from two-level atomic systems.[15] For these, one can show that under resonant coherent cw excitation, besides incoherent fluorescence emission, an elastic Rayleigh component is to be expected in the spectrum. This component originates from excited states that do not experience relaxation between absorption and emission thus resulting in a coherent coupling of the scattered signal to the exciting light. Besides being coherent, a particular advantage of resonant Rayleigh scattering is that it is a linear process which, in comparison to the nonlinear techniques mentioned above, largely facilitates the data analysis.

For resonant Rayleigh scattering to occur in *crystals*, the quasimomentum selection rule, which determines the kinematics of the elastic-scattering process, has to be at least partially lifted. This requires some kind of *disorder* which manifests itself as an inhomogeneous broadening of the electronic transition. Actually, resonance Rayleigh scattering in crystalline materials had first been observed by Hegarty *et al.* in GaAs/Al$_x$Ga$_{1-x}$As multiple-quantum-well (MQW) structures,[16] where the energetically lowest ($n = 1, e$-hh) exciton exhibits appreciable inhomogeneous broadening due to compositional disorder at the interface or in the mixed crystal barrier. Using cw excitation, in their experiments these authors

were able to nicely demonstrate the resonance enhancement of scattered Rayleigh intensity at the exciton transition.[17,18] Another reason for resonant Rayleigh scattering to occur is the roughness of the surface. This effect is well known from metallic surfaces[19] and recently was also found to occur near the direct exciton resonance in bulk CdS.[20,21]

All these investigations were restricted to measurements of the stationary response while the question of the *time dependence* of the resonant Rayleigh scattering process was left open. In the present paper, we prove both theoretically and by experiment that for excitons in disordered systems the decay of resonant Rayleigh scattering following short laser pulse excitation is characterized by a finite time constant, namely by the coherence time or, equivalently, the homogeneous width of the exciton state. Using scattering theory based on Maxwell's equations and a semiclassical dielectric susceptibility, we derive expressions for the scattered intensity both for cw and δ-pulse optical excitation. Having already reported some preliminary results,[22] we also present experimental investigations at the $(n=1,e$-hh) exciton resonance in a GaAs/Al$_x$Ga$_{1-x}$As MQW $(x=0.43)$. Using picosecond spectroscopy and measuring the time evolution of the resonant Rayleigh intensity, we are able to reveal the finite decay and, by exploiting the selection rules, to derive the coherence time and energy-relaxation time as function of exciton energy and temperature.

II. THEORY OF TIME-DEPENDENT RESONANT RAYLEIGH SCATTERING

Usually, in optical experiments such as, e.g., in Raman or Brillouin scattering, the elastic process giving rise to the Rayleigh line is a dirt effect that is caused by insufficient quality of the sample surface or bulk. It originates from spatial fluctuations in the refractive index connected with electronic resonances at much higher photon energies. The strength of the Rayleigh line in these cases is often larger by several orders of magnitude compared with that of the desired Stokes-shifted signal, and its width and tail often limit the detection of scattering signals at very low energies. In high-quality crystals, however, in which this disturbing effect is strongly reduced or can be minimized experimentally, a contribution to the Rayleigh process is detectable that is resonant with an optical transition and can provide useful information on the respective transition itself. A prerequisite for resonant Rayleigh scattering to occur is the existence of any kind of disorder in the scattering system that gives rise to spatial fluctuations in dielectric response of the material under study.

The elastically scattered intensity for this process, expected both for cw and short pulse excitation, can be derived from a strictly classical treatment of Rayleigh scattering. To this end we describe the resonant part of the dielectric function of the scattering medium by a spatially fluctuating susceptibility $\chi_S(\mathbf{r},\omega)$ that occurs in addition to the usual background susceptibility. This may be realized by a spatially dependent resonance frequency $\omega_0(\mathbf{r})$ of the transition, as, e.g., in the case of semiconduc-

tor solid solutions and quantum-well structures. The important quantities characterizing $\chi_S(\mathbf{r},\omega)$ are the distribution function of resonance frequencies denoted by $g(\omega)$ and the spatial correlation function that will be assumed to be of Gaussian form

$$\langle \chi_S^*(\mathbf{r},\omega)\chi_S(\mathbf{r},\omega')\rangle$$
$$= \langle \chi_S^*(\mathbf{r},\omega)\chi_S(\mathbf{r},\omega')\rangle_0 \exp(-|\mathbf{r}-\mathbf{r}|^2/\xi_c(\omega,\omega')^2) .$$

(2)

Here, $\langle \chi_S^*(\mathbf{r},\omega)\chi_S(\mathbf{r},\omega')\rangle_0$ is the correlation function for $\mathbf{r}=\mathbf{r}'$ and $\xi_c(\omega,\omega')$ is the correlation length which is generally frequency dependent. It characterizes the spatial extend over which coherence of the electronic states exists, a finite ξ_c showing the localized nature of the states. To avoid unnecessary computational complications, in the calculations we will disregard any influence of the surface of the scattering medium and also neglect the background susceptibility.

Being the source of the scattered field in lowest order of scattering theory (Born approximation),[23] the time-dependent dielectric polarization can be written as the time integral

$$\mathbf{P}_S(\mathbf{r},t) \propto \int_{-\infty}^{\infty} dt' \chi_S(\mathbf{r},t')\mathbf{E}_0(\mathbf{r},t-t') .$$

(3)

Here, $\chi_S(\mathbf{r},t)$ represents the Fourier transform of the spatially fluctuating resonant susceptibility $\chi_S(\mathbf{r},\omega)$. $\mathbf{E}_0(\mathbf{r},t)$ represents the electric field of the incident (laser) light wave at frequency ω_L producing the additional polarization $\mathbf{P}_S$. While having retained in Eq. (3) the temporal nonlocality of the medium, spatial nonlocality is neglected as justified for electronic states with $\xi_c < \lambda$, i.e., with spatial extension small compared to the wavelength of light, the only case that will be considered here.

Assuming the incident light field to be of form

$$\mathbf{E}_0(\mathbf{r},t) = A_0\left[t - \frac{\mathbf{r}\cdot\mathbf{k}_L}{\omega_L}\right]e^{i(\mathbf{k}_L\cdot\mathbf{r}-\omega_L t)}\cdot\mathbf{e}_L$$

(4)

$[A_0(t)$: amplitude; $\mathbf{k}_L$: wave vector; $\mathbf{e}_L$: polarization unit vector; $\mathbf{r}$: displacement vector (cf. Fig. 1)]. It is straightforward to calculate from Eq. (4) the scattered
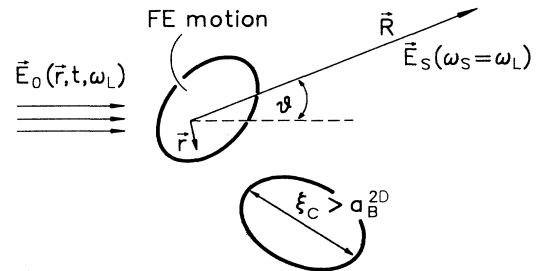

FIG. 1. Resonance Rayleigh scattering in a solid with static spatial disorder. $\mathbf{E}_0$ and $\mathbf{E}_S$ are the incident and elastically scattered electric fields with frequencies ω_L and $\omega_S=\omega_L$. In the case of quantum wells, ξ_c represents the coherence length of the electron and hole states that characterize the lateral extension of regions in which free-exciton (FE) motion parallel to the quantum-well layers is possible (see the text).

electric field $\mathbf{E}_S$ by using Maxwell's equations. Introducing the Hertz vector $\mathbf{Z}_S$,[24] it is given by

$$\mathbf{E}_S(\mathbf{r},t) = -k_L^2 \mathbf{e}_R \times [\mathbf{e}_R \times \mathbf{Z}_S(\mathbf{r},t)] \qquad (5)$$

with

$$\mathbf{Z}_S = \frac{e^{-i\omega_L(t-R/c)}}{r} \mathbf{e}_L$$
$$\times \int_{-\infty}^{\infty} e^{i\omega_L t'} A_0 \left[t - \frac{R}{c} - t' \right]$$
$$\times \left[\int_V d^3\mathbf{r}' \chi_S(\mathbf{r}'t') e^{i(\mathbf{k}_L - \mathbf{k}_S)\cdot\mathbf{r}'} \right] dt' \qquad (6)$$

[$\mathbf{e}_R$: unit vector along direction of observation $\mathbf{R}$; $\mathbf{k}_S = (\omega_L/c)\mathbf{e}_R$: wave vector of scattered light]. In deriving Eq. (5), it is assumed that the magnitude of the fluctuating part of the susceptibility is sufficiently small so that multiple-scattering processes can be neglected (validity of the Born approximation), and that the scattered wave is observed in far field (i.e., for the volume V of the scattering region small compared to the distance of the observation point) and the time variation of the field amplitude $A_0(t)$ as well as of $\chi_S(\mathbf{r},t)$ occurs on a much longer time scale than the inverse light frequency. Equation (6) represents a spherical scattered wave at frequency $\omega_S = \omega_L$ with the amplitude given by the spatial Fourier transform of the susceptibility at the scattering wave vector $\mathbf{k}_L - \mathbf{k}_S$.

If we take the frequency-dependent susceptibility to have a Lorentzian structure,

$$\chi_S(\mathbf{r},\omega) = \frac{\omega_d}{\omega_0(\mathbf{r}) - \omega - i\delta E_{\text{hom}}/2\hbar}, \qquad (7)$$

one obtains, through Fourier transformation,

$$\chi_S(\mathbf{r},t) = -i\omega_d \Theta(t) e^{-i\omega_0 t - (\delta E_{\text{hom}}/2\hbar)t}, \qquad (8)$$

where $\omega_0(\mathbf{r})$ and $\delta E_{\text{hom}} = 2\hbar/\tau_{\text{coh}}$ are the exciton resonance frequency and homogeneous linewidth, respectively, already introduced above. $\Theta(t)$ is the Heaviside step function and ω_d is a constant representing the strength of the dielectric response. Renouncing the spectral information, the scattered intensity detected at distance $\mathbf{R}$ from the scattering volume is calculated from the ensemble average $I(\mathbf{R},t) = \langle E^*(\mathbf{R},t)E(\mathbf{R},t) \rangle$. For excitation within the inhomogeneously broadened electronic transition [distribution function $g(\omega)$ of transition frequencies], one finds

$$I(\mathbf{R},t) \propto \cos^2\vartheta \xi_c^3 \exp(-|\mathbf{k}_L - \mathbf{k}_S|^2 \xi_c^2/4) g(\omega_L)$$
$$\times \int_0^\infty dt' \left| A_0 \left[t - \frac{R}{c} - t' \right] \right|^2 e^{-(\delta E_{\text{hom}}/\hbar)t'} \qquad (9)$$

with ϑ denoting the scattering angle between vectors $\mathbf{k}_L$ and $\mathbf{k}_S$ (Fig. 1). In order to derive Eq. (9) and to perform the necessary integration over the space coordinate, according to Eq. (2) the susceptibility correlation function $\langle \chi_S^*(\mathbf{r},\omega)\chi_S(\mathbf{r}',\omega') \rangle$ is taken to be of Gaussian form. One also has to presume that the correlation length ξ_c of the scattering regions is frequency independent. According

to Eq. (9), the scattered intensity shows a pronounced dependence on the scattering angle, which sensitively reflects the spatial structure of the disorder and in principle would allow us to determine its correlation length ξ_c.

Taking the incident field amplitude A_0 to be time independent as in the case of cw excitation, integration of Eq. (9) yields an intensity showing resonance enhancement inversely proportional to the homogeneous linewidth. For δ-pulse excitation the intensity becomes time dependent decaying out with time constant $\delta E_{\text{hom}}/\hbar$ or $2/\tau_{\text{coh}}$ [Eq. (1)]. Thus, measuring the decay of the resonantly scattered Rayleigh intensity enables us to determine the coherence time or homogeneous linewidth of the optical transition. We note that, in view of this result, the time dependence of the resonant Rayleigh scattering process is quite different from that expected for the specularly reflected intensity[25] which should decay with the reciprocal of the total energy width. This is due to the difference in phase relaxation of the electromagnetic waves scattered from different points of the sample. While in specular reflection all waves add up coherently due to their identical phase, in the Rayleigh process we have a statistical distribution of phases and therefore incidental superposition of the scattered waves.

III. MECHANISM AND SELECTION RULES IN MULTIPLE-QUANTUM-WELL STRUCTURES

To explain the occurrence of the resonant Rayleigh process specifically in GaAs/Al$_x$Ga$_{1-x}$As multiple quantum wells, one has to ask for the possible origin of the disorder. Because of the layered structure and restricted geometry, exciton motion in quantum wells is two dimensional with the exciton wave vector oriented parallel to the layer while localization occurs perpendicular to it. According to the model developed by us previously,[26] the quantum well may be visualized to consist of small regions in which the exciton (Bohr radius a_B^{2D}) is free to move as schematically shown in Fig. 1. The lateral extension of these regions is determined by the coherence length ξ_c (or mean free path) of the electron and hole Bloch states. Due to disorder-induced scattering, mostly at compositional fluctuations at the interface and in the mixed crystal barrier ξ_c is finite, but has to be large compared to a_B^{2D} (for GaAs quantum wells $\simeq 10$ nm) for a free exciton to exist at all. Within each of these regions, the quantum well provides an average potential for the electronic states corresponding to an effective well width $L_{z,\text{eff}}$. This, in turn, causes local differences in exciton frequency $\omega_0(\mathbf{r})$ across the sample. They are the origin of the inhomogeneous broadening of the exciton transition and, because of the strong dispersion near resonance, finally give rise to the spatial fluctuations in refractive index or susceptibility necessary for resonant Rayleigh scattering to occur.

As the exciton which is initially created in a coherent state undergoes dephasing, in any experiment one has to discriminate between coherent and incoherent processes. In the case of resonant Rayleigh scattering, the elastic processes give rise to an (incoherent) hot luminescence component at energy $E_S = E_L$. Although there has been

a long standing controversy about the discrimination of coherent scattering and incoherent hot luminescence (see, e.g., Refs. 27–30), recent theoretical work[3,31,32] has proven that under the assumption of weak coupling of the excited electronic states to a heat bath and to the light field, the decay of the coherent scattering is governed by the coherence time τ_{coh} while hot luminescence processes decay with the energy relaxation time T_1. More specifically, these conditions mean that polariton effects can be neglected which is obviously the case for the investigated GaAs quantum wells but will make similar considerations difficult in bulk GaAs or quantum wells with very narrow linewidths.

For excitons in quantum wells, in addition, one has to take into account the degeneracy of the states. Corresponding to the D_{2d} symmetry of the quantum well, the lowest ($n = 1, e$-hh) exciton is doubly degenerate (symmetry Γ_5) having transition moments along mutually orthogonal directions [110] and [$\bar{1}$10] in the plane of the quantum well.[22] Excitation with light polarized along one of these directions therefore creates the exciton in a state with well-defined polarization and phase (state $|x'\rangle$ or $|y'\rangle$, respectively; cf. Fig. 2). If the exciton is sufficiently long lived, the phase may be destroyed by elastic scattering into the degenerate state having orthogonal polarization. Clearly, the polarization of the emitted light then has lost correlation to that of the incident light even though the exciton did not undergo inelastic scattering (energy relaxation). It implies the intensity $I_\perp$ in orthogonal ("forbidden") polarization to be hot luminescence (HL) while the intensity difference $I_\parallel - I_\perp$ remaining in parallel ("allowed") polarization corresponds to coherent Rayleigh scattering (RS) originating from excitons not having experienced relaxation at all. Correspondingly, both coherent and incoherent processes contribute to $I_\parallel$ consistent with the expectation that the hot luminescence is unpolarized. In principle, there may be dephasing processes which do not lead to a depolarization, e.g., by the static disorder itself. However, in systems, where the spatial correlation length of the fluctuations is large compared to the exciton Bohr radius, no dephasing due to the disorder is expected.[33]

The time-dependent RS and HL intensities (proportional to population) are readily obtained by analyzing the exciton energy-level scheme in Fig. 2 in terms of rate equations for population. Introducing rates $1/T_2'$ and $1/T_2$ to account for elastic and inelastic scattering and solving the system of differential equations for δ-pulse excitation, one gets

$$I_{RS} = I_\parallel - I_\perp \sim \left| \sum_\alpha (\mathbf{M}_\alpha \mathbf{e}_S)(\mathbf{M}_\alpha \mathbf{e}_L) \right|^2 e^{-2t/\tau_{coh}}, \quad (10)$$

$$I_{HL} = I_\perp$$

$$\sim \frac{1}{N} \sum_{\alpha,\alpha'} |(\mathbf{M}_\alpha \mathbf{e}_S)(\mathbf{M}_{\alpha'} \mathbf{e}_L)|^2 (e^{-t/T_1} - e^{-2t/\tau_{coh}}). \quad (11)$$

In these expressions, τ_{coh} is defined as in Eq. (1) and the total-energy relaxation rate is given by $1/T_1 = \Gamma_{FE} + \Gamma_{capt}$ including radiative recombination and phonon scattering of free excitons (FE) (rate Γ_{FE}) as well as exciton capture (rate Γ_{capt}) in the localized exciton (LE) states. The prefactors are taken from a more elaborate quantum-mechanical calculation.[3] They contain the selection rules with $\mathbf{e}_L, \mathbf{e}_S$ designating the polarization unit vectors for the incident and the scattered light and $\mathbf{M}_{\alpha,\alpha'}$ the transition moments connecting the crystal ground state with exciton states $\alpha, \alpha' = |x'\rangle, |y'\rangle$. N is the number of degenerate states ($N = 2$ in the present case). According to Eqs. (10) and (11), the decay of the difference of polarized intensities directly provides τ_{coh}. $I_\perp$ then serves to separately deduce the energy relaxation time T_1 and, through Eq. (1), the pure dephasing time T_2'.

IV. EXPERIMENT

A. Setup and scattering geometry

The experimental setup which we have used is the same as described previously.[22,26] A 90° scattering geometry was chosen with the light entering the quantum-well sample under Brewster's angle ($\alpha_B \sim 75°$). Due to the large refractive index of the material ($n \simeq 3.5$), the directions of incident and scattered light propagation within the sample are oriented under angles of 15° and 4° to the surface normal which is along the growing direction $z' \| [001]$. In effect, this geometry corresponds to nearly 180° backscattering and allows the detection of $I_\parallel$ and $I_\perp$ (scattered light polarizations along $x' \| [110]$ and $y' \| [\bar{1}10]$, respectively), as required. According to Fresnel's equations, excitation under Brewster's angle with light polarized in the plane of incidence results in optimum coupling of the field into the sample and minimum reflection into the direction of observation. Therefore, the chosen geometry is most advantageous in studying polarized Rayleigh scattering.

In the picosecond pulsed measurements special precautions were met to reduce the zero-point jitter along the time scale. In each measurement a directly detected pulse transmitted via a monomode fiber to the photomultiplier tube served as a common time reference.

B. Results and analysis

The experimental results which we obtained in studying the resonant Rayleigh process in various GaAs/
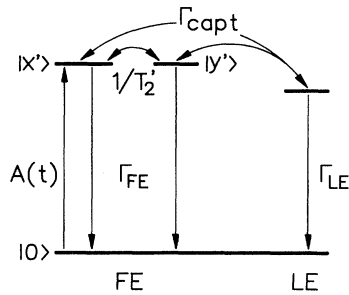

FIG. 2. Energy-level system used to analyze resonance Rayleigh scattering in GaAs/Al$_x$Ga$_{1-x}$As quantum wells. The (degenerate) free and the localized exciton states (FE, LE) are shown together with the relevant scattering processes characterized by corresponding rates as defined in the text.

$Al_xGa_{1-x}As$ multiple-quantum-well structures complete-
ly confirm the theoretical predictions in Secs. II and III.
As displayed in Fig. 3 for a sample with $x = 0.43$, under
cw excitation we observe a pronounced resonance
enhancement of the Rayleigh scattered intensity across
the $(n = 1, e\text{-hh})$ exciton. The width of the resonance is in
agreement with the inhomogeneous linewidth of the exci-
ton which in this sample is $\delta E_{inh} \approx 1.2$ meV (FWHM) as
found from independent excitation measurements. To re-
veal the resonant contribution to the elastically scattered
intensity, the excitation beam was focused down to a
small spot of about 50 μm in diameter. Simultaneously,
its intensity was reduced to less than 0.1 W/cm^2 power
density to avoid high excitation effects. The spot at the
sample surface was imaged onto a charge coupled device
(CCD) camera and scanned across the sample to find lo-
cations where scattering outside the exciton resonance
was as weak as possible. Compared to "usual" excitation
conditions (see, e.g., the inset of Fig. 6), the low laser
power changes the appearance of the spectrum quite
drastically. It brings up the intensity of the localized ex-
citon (LE) relative to that of the free exciton (FE) which
occurs mostly concentrated around the resonance Ray-
leigh peak. The spectral width of the exciting laser was
$\delta E_L < 0.02$ meV, i.e., small compared to the homogene-
ous linewidth (see below). Under this condition, the Ray-
leigh linewidth, in principle, is determined by δE_L,[15] the

larger width seen in the spectra coming from the spectral
resolution of the monochromator as we had to open up
the slits for reasons of intensity. Depending on the
different sample quality, we have found enhancements in
integrated intensity by a factor 20 to 50 relative to the
nonresonant case.

Employing the selection rules of Sec. III, the spectra in
Fig. 3 were measured with differently polarized light. As
implied by the Rayleigh line intensity showing up in "for-
bidden" polarization $(I_\perp)$, considerable depolarization
occurs. It depends on excitation photon energy and gives
rise to a variation in polarization degree $[P = (I_\parallel - I_\perp)/(I_\parallel + I_\perp)]$ between 0.85 at the high-energy side of
the FE and complete depolarization in the LE region (see
Fig. 3). Because the resonance enhancement at the exci-
ton originates from the combined effects of absorption
and homogeneous linewidth [cf. Eq. (9)], absolute mea-
surements of scattering intensities would be necessary to
determine the homogeneous linewidth or the coherence
time from cw experiments.

Using picosecond pulses for excitation and time-
resolved spectroscopy having sufficient time resolution,
we were able to prove experimentally the predicted finite
decay time of the resonant Rayleigh process which could
not be revealed before. Figure 4 illustrates decay curves
for the two orthogonal polarizations together with the
system response to the laser pulse (L) which had an actu-
al width of 5 ps measured by its autocorrelation. The im-
portant feature is the fast process in parallel polarization
which decays out in about 60 ps, but clearly is delayed
relative to the laser. The slow decay at longer times
found in both $I_\parallel$ and $I_\perp$ (decay times ~ 150 ps at 2 K) is
due to thermally activated reemission from the LE states
and will be described in a separate paper. To more clear-
ly demonstrate the time decay of the Rayleigh process, in
Fig. 5 we plot the time-dependent difference $I_\parallel - I_\perp$ on an
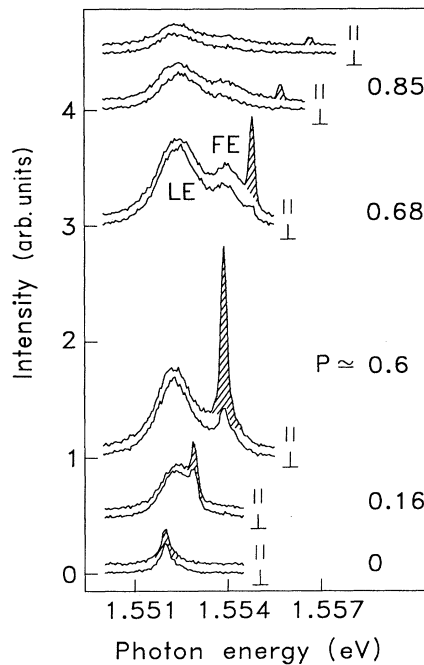

FIG. 3. Resonance enhancement of the Rayleigh-scattered
intensity for cw laser excitation across the $n = 1, e$-hh free exci-
ton (FE) in a GaAs/$Al_xGa_{1-x}As$ ($x = 0.43$) quantum well. The
sample consists of three wells with well and barrier widths of
$L_z = 9$ nm and $L_b = 105$ nm. The incident light polarization is
$e_L \| [110]$. $I_\parallel$ and $I_\perp$ correspond to scattered light polarizations
$e_S \| [110]$ and $[\bar{1}10]$, respectively. LE denotes luminescence
from localized exciton states not discussed here. $T = 2$ K. P is
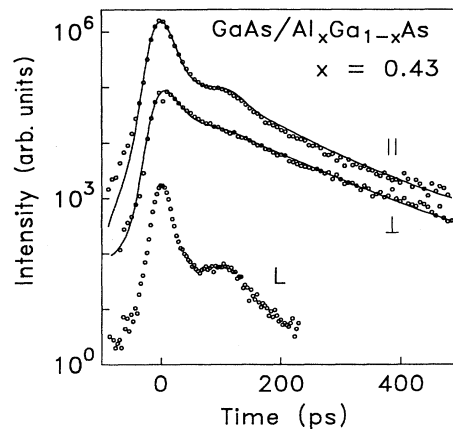the degree of polarization at $\omega_L = \omega_S$.

FIG. 4. Polarized transient resonant Rayleigh scattering for
the sample in Fig. 3 excited in the exciton absorption peak at
$E_0 = 1.555$ eV. The full lines are fits to the experimental data
(points); for clearer representation the curves are shifted along
the ordinate. The slow decay at longer times is due to thermal
reactivation of localized into free exciton states. L: system
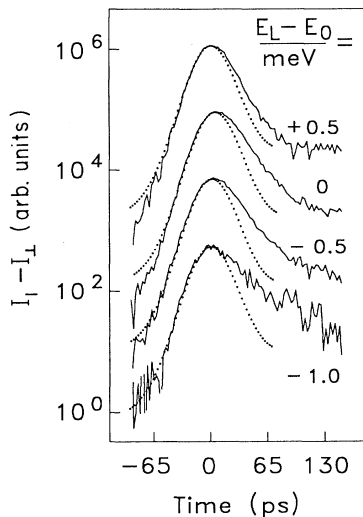response to the laser pulse measured off resonance. $T = 2$ K.

FIG. 5. Time decay of the coherent contribution to the Rayleigh intensity at 2 K. The normalized intensity difference for two orthogonal polarizations is plotted vs time. Excitation at various energies E_L around the exciton peak E_0. Dotted curve: system response to the laser pulse off resonance.
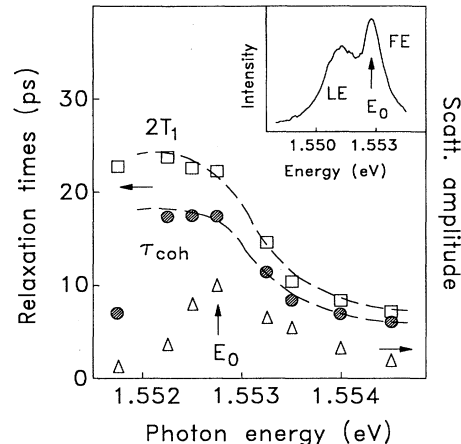

FIG. 6. Coherence time and energy-relaxation time as function of energy in the exciton region as derived from the experimental data. The dashed lines are guide lines for the eye. Also shown is the scattering amplitude (open triangles). Inset: free and localized exciton spectrum (FE, LE) at 2 K.

extended time scale. According to Eq. (10), this representation directly reveals the coherent Rayleigh contribution that decays with τ_{coh} while the intensities at longer times cancel. The decay curves are shown for slightly different excitation energies around the exciton resonance at E_0. They are normalized and represented together with the response to the exciting laser. In comparison with the cw spectra in Fig. 3, in the time-resolved measurement the spectral width of the exciting laser was broader ($\delta E_L \simeq 0.3$ meV) to reduce its temporal width and have sufficiently good time resolution.

The analysis of these measurements provides the various relaxation times (Sec. III). The data obtained from a series of measurements in which the excitation photon energy (E_L) was systematically varied across the free-exciton transition are summarized in Fig. 6. Both τ_{coh} and T_1 strongly depend on exciton energy. Due to the increasing number of relaxation processes at higher energies, τ_{coh} decreases from about 20 ps to about 6 ps which is presently the detection limit of our setup. This corresponds to values of the homogeneous linewidth 0.06 $\leq \delta E_{hom} \leq 0.22$ meV, i.e., smaller by a factor of 10 compared to the inhomogeneous width of the exciton line. These values are in good agreement with results obtained in similar samples by nonlinear techniques.[2,34] In particular they are consistent with the assumption of noncoherence of the spatially separated exciton states (cf. Sec. III) as the dephasing connected with the inhomogeneous broadening would correspondingly result in a decay about ten times fast. Also, the scattering amplitude that follows from the analysis (see Fig. 6) quite nicely reproduces the exciton line shape and width.

To test the quality of our analysis, we used the theoretical time dependences of $I_{\parallel}$ and $I_{\perp}$ to fit the experimental decay curves. The full lines in Fig. 4 show an example.

For the fit we took the corresponding set of relaxation times and performed a convolution with the measured system response to the laser pulse. Similar fits were performed for other excitation energies all giving very good agreement.

Comparison of the relaxation times in Fig. 6 with Eq. (1) suggests that the exciton coherence is predominantly destroyed by inelastic-scattering processes characterized by rate $1/T_1$. Nearly independent of exciton energy, pure dephasing (rate $1/T_2'$) contributes with about 20–25 % to the homogeneous linewidth. For excitation in the exciton resonance at energy E_0, we have also studied the temperature dependence of the decay and found a linear increase of δE_{hom} with temperature between 2 and 17 K. It suggests that the exciton-phonon interaction is predominantly governed by LA phonons via deformation-potential coupling. Quantitatively, however, the scattering rate is larger than expected on the basis of theoretical calculations[26] which may be due to nonconservation of the k vector induced by the static disorder.

V. CONCLUDING REMARKS

As demonstrated theoretically and experimentally in this paper, resonant Rayleigh scattering represents a very direct and powerful method for measuring the homogeneous linewidth and provides detailed knowledge on exciton dynamics. The relevant information is contained in the resonant contribution to the elastically scattered intensity which usually is obscured by a large nonresonant part. As already pointed out, in this respect it is similar to other types of light-scattering processes such as Raman and Brillouin scattering or quasielastic critical light scattering. The mechanisms for these processes, however, are of quite different origin because in these cases dynamical fluctuations either in the phonon field or in entropy give

rise to the scattered signal. Distinctly different from this, a prerequisite for resonance Rayleigh scattering is a spatial *static* disorder of the investigated system as in the heterostructures described in this paper. As such, this method generally is applicable to investigate the relaxation properties of electronic states in disordered systems and in particular works at very low intensities where nonlinear techniques become problematic.

---

[1] J. Lumin. **36**, 179 (1987).

[2] J. Kuhl, A. Honold, L. Schultheis, and C. W. Tu, Festkörperprobleme **29**, 157 (1989).

[3] H. Stolz, in *Festkörperproblem/Advances in Solid State Physics XXXI*, edited by U. Rössler (Pergamon, Vieweg, 1991), p. 219.

[4] L. Schultheis, A. Honold, J. Kuhl, K. Köhler, and C. W. Tu, Phys. Rev. B **34**, 9027 (1986).

[5] E. O. Göbel, K. Leo, T. C. Damen, J. Shah, S. Schmid-Rink, W. Schäfer, J. F. Müller, and K. Köhler, Phys. Rev. Lett. **64**, 1801 (1990).

[6] B. F. Feuerbacher, J. Kuhl, R. Ecleston, and K. Ploog, Solid State Commun. **74**, 1279 (1990).

[7] K. Leo, T. C. Damen, J. Shah, E. O. Göbel, and K. Köhler, Appl. Phys. Lett. **57**, 19 (1990).

[8] P. C. Becker, H. L. Fragnito, C. H. Cruz, R. L. Fork, J. E. Cunningham, J. E. Henry, and C. V. Shank, Phys. Rev. Lett. **61**, 1647 (1988).

[9] G. Noll, U. Siegner, S. G. Shevel, and E. O. Göbel, Phys. Rev. Lett. **64**, 792 (1990).

[10] B. Fluegel, N. Peyghambarian, G. Olbright, M. Lindberg, S. W. Koch, M. Joffre, D. Hulin, A. Migus, and A. Antonetti, Phys. Rev. Lett. **59**, 2588 (1987).

[11] V. Langer, H. Stolz, and W. von der Osten, J. Lumin. **45**, 406 (1990); Phys. Rev. Lett. **67**, 679 (1991).

[12] W. A. J. A. Van der Poel, A. L. G. J. Severens, and C. T. Foxon, Opt. Commun. **76**, 116 (1990).

[13] S. Bar-Ad and I. Bar-Joseph, Phys. Rev. Lett. **66**, 2491 (1991).

[14] H. Stolz, V. Langer, E. Schreiber, S. Permogorov, and W. von der Osten, Phys. Rev. Lett. **67**, 679 (1991).

[15] R. Loudon, *The Quantum Theory of Light* 2nd ed. (Clarendon, Oxford, 1986).

[16] J. Hegarty, M. D. Sturge, C. Weisbuch, A. C. Gossard, and W. Wiegmann, Phys. Rev. Lett. **49**, 930 (1982).

[17] J. Hegarty, L. Goldner, and M. D. Sturge, Phys. Rev. B **30**, 7346 (1984).

[18] J. Hegarty and M. D. Sturge, J. Opt. Soc. Am. B **2**, 1143 (1985).

[19] A. A. Maradudin and D. L. Mills, Phys. Rev. B **11**, 1392 (1975).

[20] V. A. Kosobukin and A. V. Sel'kin, Solid State Commun. **66**, 313 (1988).

[21] V. A. Kosobukin, M. I. Sazhin, and A. V. Sel'kin, Fiz. Tverd. Tela (Leningrad) **32**, 1023 (1990) [Sov. Phys. Solid State **32**, 602 (1990)].

[22] H. Stolz, D. Schwarze, W. von der Osten, and G. Weimann, Superlatt. Microstruct. **9**, 511 (1991).

[23] J. D. Jackson, *Klassische Elektrodynamik* (de Gruyter, Berlin, 1983).

[24] B. Crosignani, P. Di Porto, and M. Bertolotti, in *Statistical Properties of Scattered Light*, edited by Yoh-Han Pao (Academic, New York, 1975), p. 54.

[25] J. Aaviksoo and J. Kuhl, IEEE J. Quantum Electron. **25**, 2523 (1989).

[26] H. Stolz, D. Schwarze, W. von der Osten, and G. Weimann, Superlatt. Microstruct. **6**, 271 (1989).

[27] Y. R. Shen, Phys. Rev. B **14**, 1772 (1976).

[28] Y. Toyozawa, J. Phys. Soc. Jpn. **41**, 400 (1976).

[29] R. Solin and H. Merkelo, Phys. Rev. B **14**, 1775 (1976).

[30] E. Courtens and A. Szöke, Phys. Rev. A **15**, 1588 (1977).

[31] K. Maruyama, F. Shibata, and M. Aihara, Physica A **153**, 441 (1988).

[32] T. Kushida and S. Kinoshita, Phys. Rev. A **41**, 6042 (1990).

[33] D. Bennhardt, P. Thomas, A. Weller, M. Lindberg, and S. W. Koch, Phys. Rev. B **43**, 8934 (1991).

[34] M. D. Webb, S. T. Cundiff, and D. G. Steel, Phys. Rev. Lett. **66**, 934 (1991); Phys. Rev. B **43**, 12 658 (1991).